Modeling and Analysis Techniques for Suspension Rubber Bushings

Satoshi Ito*, Taro Koishikura*, and Daichi Suzuki**

*Toyota Motor Corporation

**Toyota Technical Development Corporation

Abstract: Suspension rubber bushings in full vehicle models are usually represented with nonlinear spring elements. However, when bushings are preloaded or deformed in diagonal direction, the spring element models tend to express inaccurate movement. In this paper, suspension rubber bushings are modeled with solid finite elements. We established a technique enabling to evaluate the nonlinear large deformation behavior of rubber bushings. This modeling technique is also able to improve simulation accuracy compared to the conventional modeling technique.

Keywords: Experimental Verification, Hyperelasticity, Rubber Bushing

1. Introduction

Recently, the performance enhancement of computers is remarkable with the progress of computer technologies. Computer simulations for the behavior of car suspensions can be done in a large-scale suspension assembly level. In assembly analyses, the accuracy in the behavior of the connecting parts becomes more important as it influences the analysis results of the entire suspension. Rubber bushings are frequently used in a suspension assembly (See FigureA1 in Appendix). Bushings are usually modeled simply with nonlinear scalar spring elements in CAE analyses. But in some cases, spring models cannot express accurate movement of suspension parts.

There are various reports in which experimental techniques are introduced to accurately evaluate the fatigue strength of bushings and the input load to the arm [1, 2]. In this paper, the issues of the nonlinear spring model are concretely shown, and the technique for solving them is described.

2. Issues of nonlinear spring model

2.1 Influence of preload to rotational stiffness

As an example, we take the case where axial force and moment are applied simultaneously to a cylindrical bushing as shown in Figure 1. When the axial force A is applied to the arm first, then the rotational spring stiffness under the moment B becomes stiffer than the one without the preloading. However, this phenomenon cannot be modeled by a combination of individual nonlinear springs since the six degrees of freedom are uncoupled.

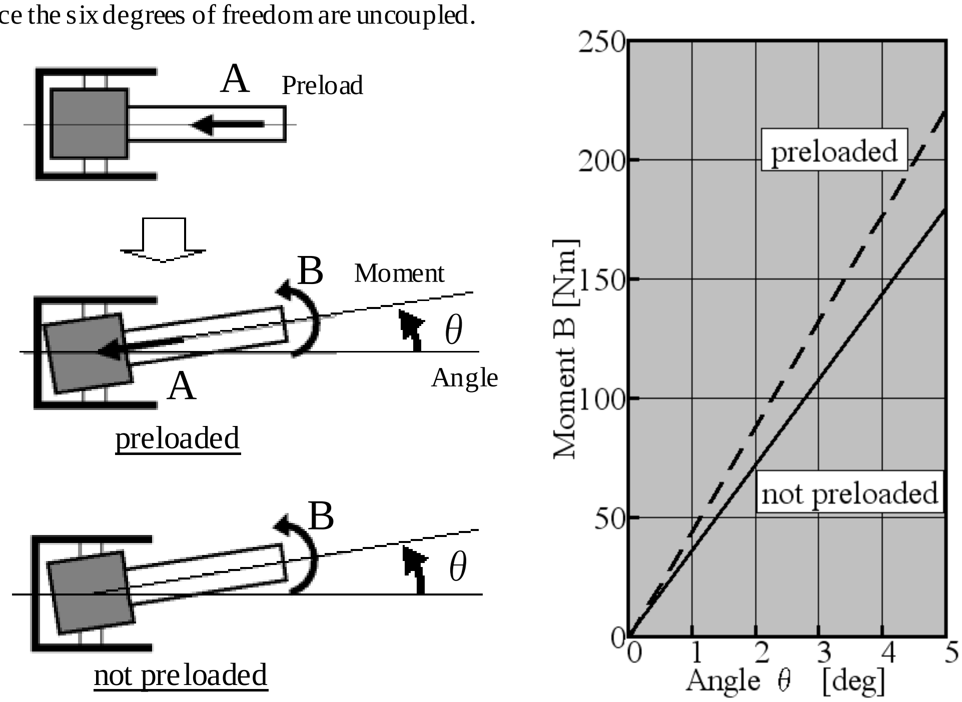

Figure 1. Influence of preload to rotational stiffness

2.2 Non linear deformation behavior in diagonal direction

Figure 2 shows a bushing with two slots. Direction B in the figure indicates the direction in which the slots are open or closed, direction A is normal to direction B, and direction C is in diagonal 45 degrees.

The stiffness of the bushing is softer in direction B than that in direction A. So, it is expected that the stiffness in direction C takes a value between that of direction A and direction B.

However, the actual stiffness in direction C cannot be evaluated by a simple combination of the nonlinear springs in direction A and B as shown in Figure 3. Although the stiffness in direction C is between that of direction A and B in the linear range, in the nonlinear range, the stiffness in direction C falls below the stiffness of direction B.

This fact decreases the accuracy of the simulation of the simple nonlinear spring model and shows why more accurate bushing modeling techniques are needed.

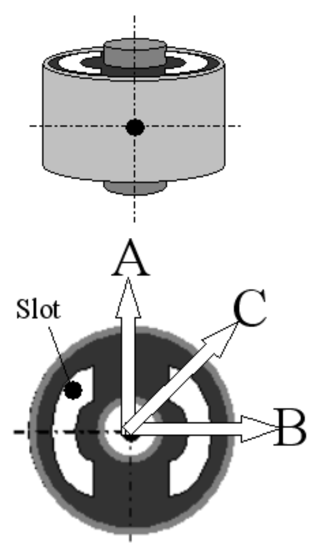

Figure 2. Bushing directions

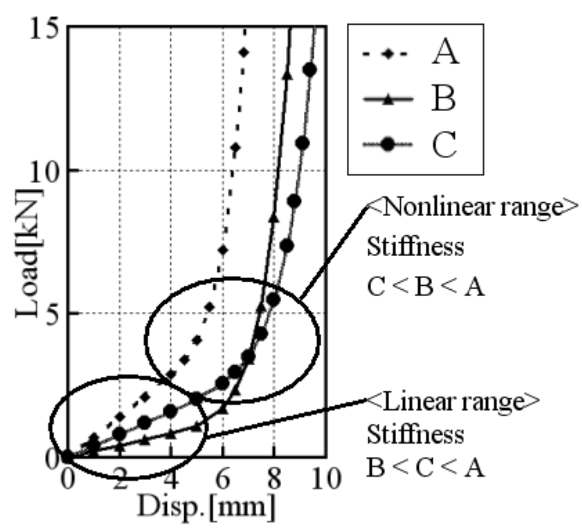

Figure 3. Load-displacement curves

.

3. Detailed FEM model for Bushing

3.1 Detailed FEM model

To resolve the issues described in the preceding chapter, a detailed FEM model was constructed.

(1) Geometry modeling

CAD was used to represent the global geometry. On the other hand the laser scan technology was applied to catch complex geometries accurately. Figure 4 shows an example.

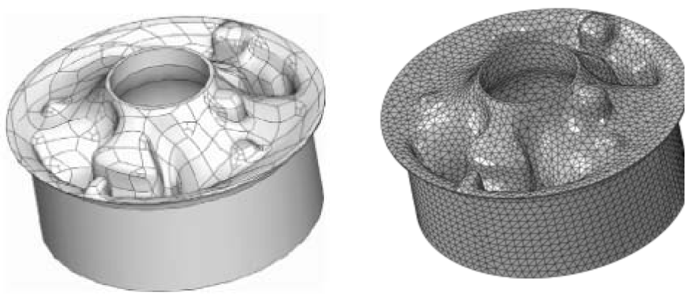

Laser scanned geometry Meshing model

Figure 4. Example of bushing model

(2) Material modeling

Generally, rubber materials are approximated as incompressible, elastic and isotropic. The behavior of such materials is shown by strain energy potential. Various material models for rubber have been proposed since the 1930's [3].

Many models require material test data for fitting. But "direct test data input" is somewhat inconvenient to manipulate in the correlation process, so we chose to use the Yeoh model based solely on material constants. There is a clear relation between the material parameter and the physical characteristic as described in the following. We used this relation for the material property definition.

(3) Material parameters

The strain energy potential of the Yeoh model is written as:

$$U = \sum_{i=1}^{3} C_{i0}\left(\overline{I}_1 - 3\right)^{i} + \sum_{i=1}^{3} \frac{1}{D_i}\left(J_{el} - 1\right)^{2i}$$

where $\overline{I}_1$ is the first deviatoric strain invariant and J_{el} is the volume ratio by elastic deformation. In the Yeoh model, the initial shear modulus μ_0 and the bulk modulus K are given as follows by the material constants C_{10} and D_1 ;

$$\mu_0 = 2\,C_{10}, \qquad K = 2/\,D_1$$

Here, the initial shear modulus determines the coefficient C_{10}, and the bulk compressibility gives the value D_1.

We performed material experiments and found that the hardness and the initial shear modulus of filled rubber are loosely related. Based on this relation, C_{10} is able to be evaluated easily according to the hardness of rubber as shown in Figure 5.

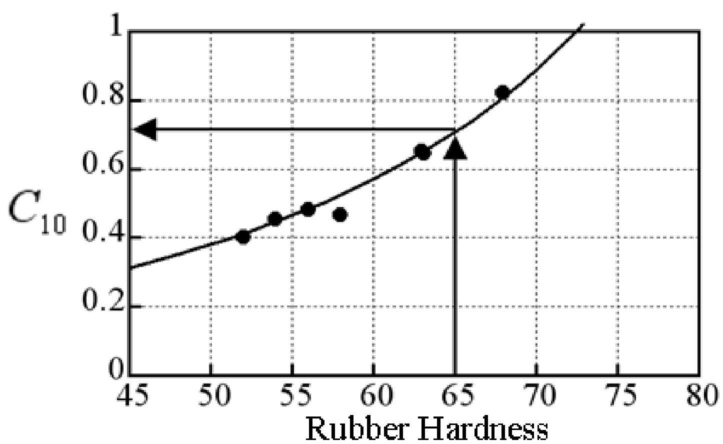

Figure 5. Relation between C_{10} and rubber hardness

.

3.2 Selection of calculation method

The rubber part can self-contact when the bushing is subjected to large deformation. In such cases, the implicit method occasionally fails to get a converged solution and does not give the results at the targeted load level. In this paper, the Explicit-method was adopted, and in consequence the calculation range was extended to the area where the load rapidly stands up as shown in Figure 6.

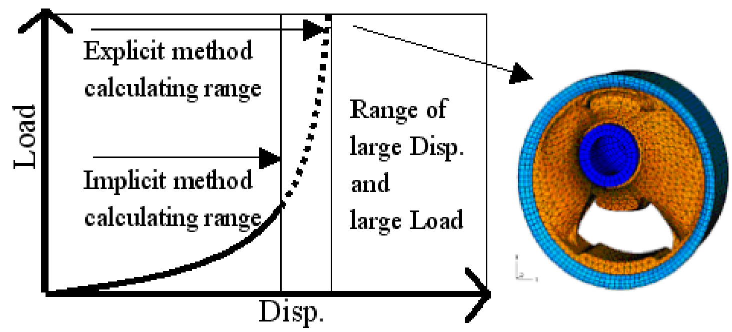

Figure 6. Range where each method is applicable

In a quasi-static analysis, a mass scaling technique was employed to speed up the simulation and reduce the computational costs. The kinetic energy was monitored to ensure that the ratio of kinetic energy compared to internal energy did not get too large (See Figure7).

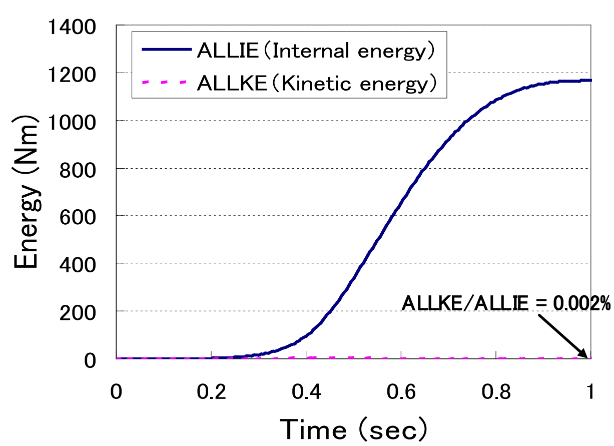

Figure 7. Comparison of ALLIE and ALLKE

4. Accuracy validation

The rotational stiffness were calculated under two levels of preload which was applied in normal direction to the bushing axis as shown in Figure 8, and the results were compared with the measurement. Figure 9 shows the results. The rotational stiffness increases as the preloading level increases, and this correlates very well with the test results. Figure 10 shows the deformed shapes. The slot is open when the preload level is 0 and the rotational stiffness is almost constant. However the slot closes when the preload is 8kN and 18kN, and the rotational stiffness changes greatly.

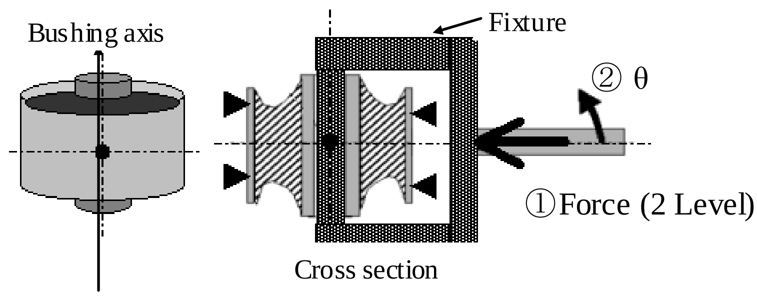

Figure 8. Measurement of rotational stiffness under preload

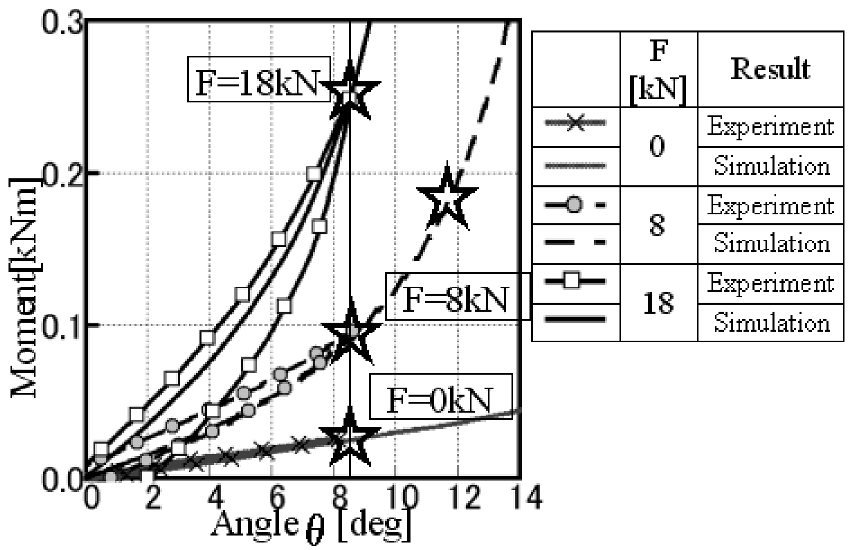

Figure 9. Moment-angle curve

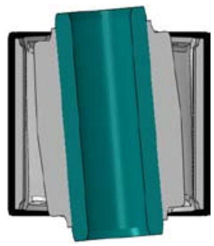

F=0kN, θ =8.5deg

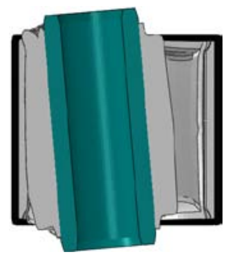

F=8kN, θ =8.5deg

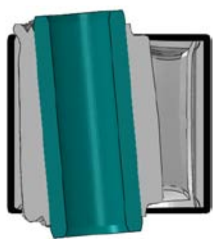

F=18kN, θ =8.5deg

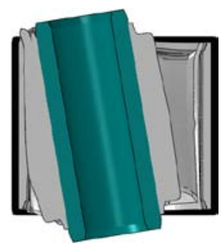

F=8kN, θ =11.5deg

Figure 10. Deformed shapes with preloads

5. Conclusions

The issue due to the nonlinear spring model was shown in the strength and deformation analyses of suspension systems.

To solve the issue, the bushing was represented by solid elements.

An appropriate and simple method was proposed to define the material constants of rubber bushing material.

It was confirmed that Explicit method simulation is more stable compared with the implicit method in dealing with strong nonlinear behaviors of bushings.

The simulation results correlate very well to those in the tests in large deformation range and it was shown that the rotational stiffness increase with the increase in preload level.

These techniques will be applied to the suspension assembly simulation in the future.

6. References

1. Dae-Un, S., Gi-Seob, J., Sang-Gun, J.: An integrated Approach to the Development of Suspension Rubber Bushings, SAE TECHNICAL PAPER SERIES, 2006-01-1623
2. Stephen, W., Gustavo, N., Alexandre, P.: Lower Control Arm Rear Bushing Development An Integrated Approach, SAE TECHNICAL PAPER SERIES, 2003-01-3676
3. Marckmann, G., Verron E.: Comparison of hyperelastic models for rubber-like materials,Rubber Chemistry and Technology Vol.79(5),2006, p.847

7. Appendix

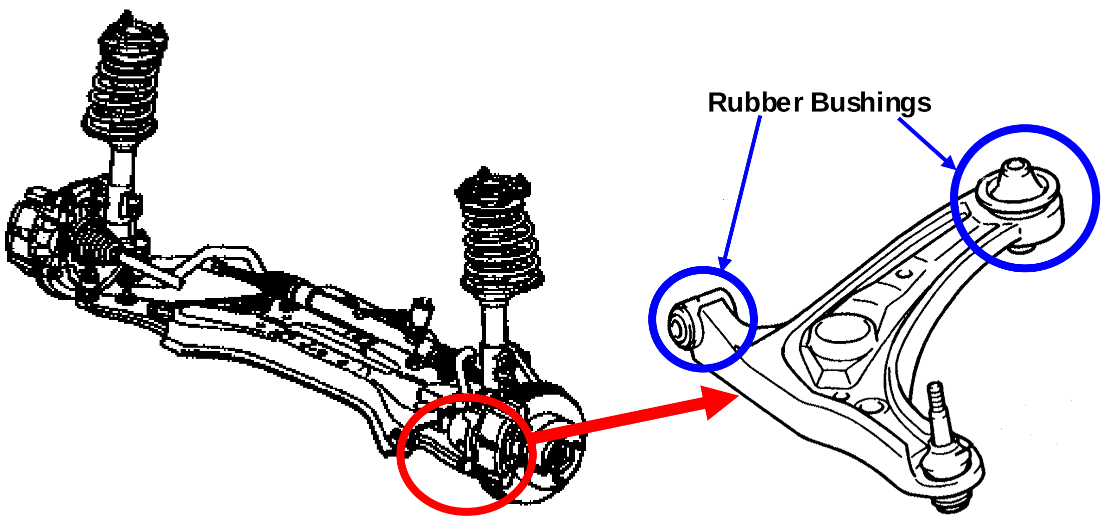

Figure A1. Suspension Assembly and Rubber Bushings

8. Acknowledgement

The authors are grateful for the support of Noriko Ohtsuka, Izumi Kato of Toyota Technical Development Corporation, and Tod Dalrymple, Jaehwan Choi, Masataka Katayama of Dassault Systems Simulia Corp.

The authors are also pleased to everyone who helped review and correct this paper to make it better. Thank you.